

Impact of perfusion on neuronal development in human derived neuronal networks

Cite as: APL Bioeng. 8, 046102 (2024); doi: 10.1063/5.0221911

Submitted: 4 June 2024 · Accepted: 18 September 2024 ·

Published Online: 1 October 2024



View Online



Export Citation



CrossMark

Donatella Di Lisa,^{1,2,3,a)}  Andrea Andolfi,¹ Giacomo Masi,¹  Giuseppe Uras,^{4,5}  Pier Francesco Ferrari,^{6,7} Sergio Martinoia,^{1,3}  and Laura Pastorino^{1,2,3,a)} 

AFFILIATIONS

¹DIBRIS, Department of Informatics, Bioengineering, Robotics and Systems Engineering, University of Genoa, Via Opera Pia 13, 16145 Genoa, Italy

²IRCCS Ospedale Policlinico San Martino, Largo Rosanna Benzi 10, 16132 Genoa, Italy

³Inter-University Center for the Promotion of the 3Rs Principles in Teaching & Research (Centro 3R), Genoa, Italy

⁴Department of Movement and Clinical Neuroscience, Institute of Neurology, Royal free Hospital, London, United Kingdom

⁵Dipartimento di Scienze Biomediche, Università degli studi di Sassari, Sassari, Italy

⁶Department of Civil, Chemical and Environmental Engineering, University of Genoa, via Opera Pia, 15, Genoa, Italy

⁷Research Center of Biologically Inspired Engineering in Vascular Medicine and Longevity, University of Genoa, via Montallegro, 1, Genoa, Italy

^{a)} Author to whom correspondence should be addressed: laura.pastorino@unige.it and Donatella.dilisa@edu.unige.it

ABSTRACT

Advanced *in vitro* models of the brain have evolved in recent years from traditional two-dimensional (2D) ones, based on rodent derived cells, to three-dimensional (3D) ones, based on human neurons derived from induced pluripotent stem cells. To address the dynamic changes of the tissue microenvironment, bioreactors are used to control the *in vitro* microenvironment for viability, repeatability, and standardization. However, in neuronal tissue engineering, bioreactors have primarily been used for cell expansion purposes, while microfluidic systems have mainly been employed for culturing organoids. In this study, we explored the use of a commercial perfusion bioreactor to control the culture microenvironment of neuronal cells in both 2D and 3D cultures. Namely, neurons differentiated from human induced pluripotent stem cells (iNeurons) were cultured in 2D under different constant flow rates for 72 h. The impact of different flow rates on early-stage neuronal development and synaptogenesis was assessed by morphometric characterization and synaptic analysis. Based on these results, two involving variable flow rates were developed and applied again in 2D culture. The most effective protocol, in terms of positive impact on neuronal development, was then used for a preliminary study on the application of dynamic culturing conditions to neuronal cells in 3D. To this purpose, both iNeurons, co-cultured with astrocytes, and the human neuroblastoma cells SH-SY5Y were embedded into a hydrogel and maintained under perfusion for up to 28 days. A qualitative evaluation by immunocytochemistry and confocal microscopy was carried out to assess cell morphology and the formation of a 3D neuronal network.

© 2024 Author(s). All article content, except where otherwise noted, is licensed under a Creative Commons Attribution-NonCommercial 4.0 International (CC BY-NC) license (<https://creativecommons.org/licenses/by-nc/4.0/>). <https://doi.org/10.1063/5.0221911>

INTRODUCTION

Traditional preclinical models of the brain, namely, two-dimensional (2D) *in vitro* cultures and animal models, have demonstrated limitations over the years in producing clinically translatable results.^{1,2} This is mainly due to the oversimplicity of 2D *in vitro* cultures and the interspecies differences between humans and non-human mammals.^{3,4} In this context, in the last few years, the need for more reliable, readily available, and reproducible preclinical models has emerged. Consequently, a great effort is currently devoted to developing

advanced brain *in vitro* models that mimic the *in vivo* brain microenvironment.⁵ Indeed, this is a challenging task due to the high complexity of the brain and the approach followed is that of developing a specific model for each specific need. However, some fundamental aspects must always be considered, such as the use of human relevant cellular phenotypes, the recapitulation of the cellular micro physiological environment, and the adoption of dynamic culture conditions.^{6,7}

In this sense, the advent of human induced pluripotent stem cells (h-iPSCs) has made possible to generate neuronal cells from donors,

including patients providing the opportunity to study *in vitro* physiological processes, such as neurodevelopment, and diseases, such as neurodegenerative ones.^{8,9} Moreover, even if 2D *in vitro* cultures still remain indispensable to model some aspects of the nervous system, such as neurite outgrowth, they are widely recognized as oversimplified. This is because they fail to account for the complex and pivotal role of the extracellular matrix (ECM) in guiding and influencing cell differentiation, growth, and communication. The recapitulation of the cellular micro-physiological environment so far has been achieved by coupling three-dimensional (3D) scaffolds, based on decellularized brain ECM or synthetic ECM-like matrix, to nervous cells.^{10,11}

Finally, conventional 2D and 3D cultures are typically maintained under static conditions, which limit the transport of nutrients, oxygen, and waste, requiring periodic replacement of the culture media.^{12–14} This leads to continuous changes in the chemical environment over time, with nutrients depleting and toxic metabolites accumulating. This situation does not mimic the *in vivo* environment, where most cells are constantly exposed to a fresh supply of nutrients and waste products are removed via the circulatory system. Additionally, chemical signaling is essential in stem cell differentiation, meaning that a constant and homogeneous distribution of signaling molecules is desirable.^{15,16} Another limitation of static cultures is the absence of mechanical stimulation, such as shear stress, which is essential *in vivo* for driving cell differentiation, growth, and tissue maturation. Mechanical stimuli activate specific ion channels, such as Piezo ones, regulate gene transcription, and direct the alignment of cytoskeletal proteins in both healthy and diseased cells.¹⁷ In the literature, it has been reported how neurogenesis and neural regeneration may be also driven by mechanical factors. In this view, the contribution of flow-induced shear stress could play a pivotal role in the development of mature and functional neuronal networks.^{17–19}

To overcome the limitations of static conditions, dynamic culture protocols based on the use of bioreactors have been developed over the years. Among the different bioreactors configurations, perfusion systems are the most utilized in tissue engineering.^{20,21} With this configuration, the culture is placed directly within the vessel through which the media continuously flows, with a flow rate determining the shear forces experienced by the cells. However, bioreactors have been successfully used mainly for cardiac, bone, cartilage, and vascular tissues, as well as for stem cell studies, whereas little attention given to fluid flow during neuronal cell culture. In this respect, suspension bioreactors, such as stirred tanks, have been used for neural and stem cells expansion,²² whereas perfusion systems are mainly applied in microfluidic devices for 2D, 3D scaffold based, and organoids cultures. Indeed, microfluidic devices have been widely used to engineer brain circuits, support organoid cultures, and develop brain-on-a-chip systems.^{23,24} However, microfluidic devices are usually custom made with specific designs and are made by polydimethylsiloxane, which can absorb different substances, reducing the reliability and reproducibility of some tests.^{25,26} Additionally, microfluidic devices support the culture of low-density networks, and their coupling with certain experimental measurements could be challenging.

In the view of developing a readily available platform to model the brain tissue *in vitro*, we have developed a protocol for the dynamic culture of nervous cells in both 2D and 3D configurations using a commercial perfusion bioreactor. For this purpose, neurons differentiated from h-iPSCs, and the human neuroblastoma SH-SY5Y cell line,

commonly used as Parkinson's disease model,²⁷ were used as physiological and pathophysiological models, respectively. As a first step, the protocol for the 2D cultures under perfusion was optimized in terms of flow rates to enhance neuronal growth and maturation compared to standard static cultures. To carry out this evaluation, the well-established model introduced by Dotti *et al.* for the polarization process of neurons²⁸ was used. Namely, the number of neuritic processes including primary, secondary, and tertiary processes, their length, and the growth rate of the major process were assessed. Moreover, a functional analysis was performed through synaptic counting. Finally, the optimized perfusion protocol was applied to 3D neuronal cultures, obtained by encapsulating nervous cells into a chitosan-based thermogel. Both neurons differentiated from h-iPSCs and SH-SY5Y neuroblastoma cells were used. The cultures were preliminary characterized from a morphological point of view in both static and dynamic cultures by immunolabeling and confocal microscopy.

RESULTS

To assess how perfusion affects cell development in human neuronal cells, as a first step, we carried out morphometric and morphological characterizations under both *static* and *dynamic* conditions. Specifically, 2D cell cultures were exposed to both *constant* and *variable flow* conditions during the culture period to evaluate the positive effect of the perfusion on neuronal cell growth and development. *Constant flow* refers to continuous perfusion at a fixed flow rate from day 0 throughout the culture period. In contrast, *variable flow* involves adjusting the flow rate every 24 h during the initial 3 days of culture, which are critical for early-stage neuronal development.

Morphometric characterization under *constant flow*

Neuronal cells, in both *static* and *dynamic* conditions at a *constant flow rate* [100, 120, and 150 $\mu\text{l}/\text{min}$; Fig. 1(a)], followed the Dotti model, and the number of neurites per cell increased during the whole culture period [Fig. 1(b)]. Four hours after plating, before perfusion, iNeurons exhibited a cell soma surrounded by lamellipodia. After 24 h, the lamellipodia of iNeurons transformed into distinct short neuritic processes. These can be defined as neurites since they are well-recognizable processes with a length equal to or greater than the diameter of the cell body. By the second day in culture, most cells showed a significantly elongated process compared to others, though it was not yet long enough to be identified as an axon. To be classified as an axon, a neuritic process must have a length equal to or greater than 80–100 μm . After 72 h in culture, the major process lengthened further; in the meanwhile, secondary processes started to grow, and tertiary processes appeared. This qualitative analysis was confirmed and further investigated with quantitative evaluation. The first evaluation took into consideration the average number of total neurites per cell [Fig. 1(c)]; 4 h after plating, the average number of processes was found to be 1.55 ± 1.64 . After that, in the *static cultures*, the number of processes gradually rose over time. In dynamic cultures, at 100 $\mu\text{l}/\text{min}$, the average number of neurites did not significantly show variation over the time. In dynamic cultures at 120 and 150 $\mu\text{l}/\text{min}$, a decrease in the number of neurites was observed instead with the increase in the flow rate, Fig. 1(c). In *static* and *dynamic cultures* (120 $\mu\text{l}/\text{min}$) at 24 h, neurons showed a similar trend, with a number of neurites of 3.60 ± 1.90 and 4.13 ± 2.48 , respectively; meanwhile, the number of neurites for neurons exposed to a flow rate of 120 $\mu\text{l}/\text{min}$ decreased,

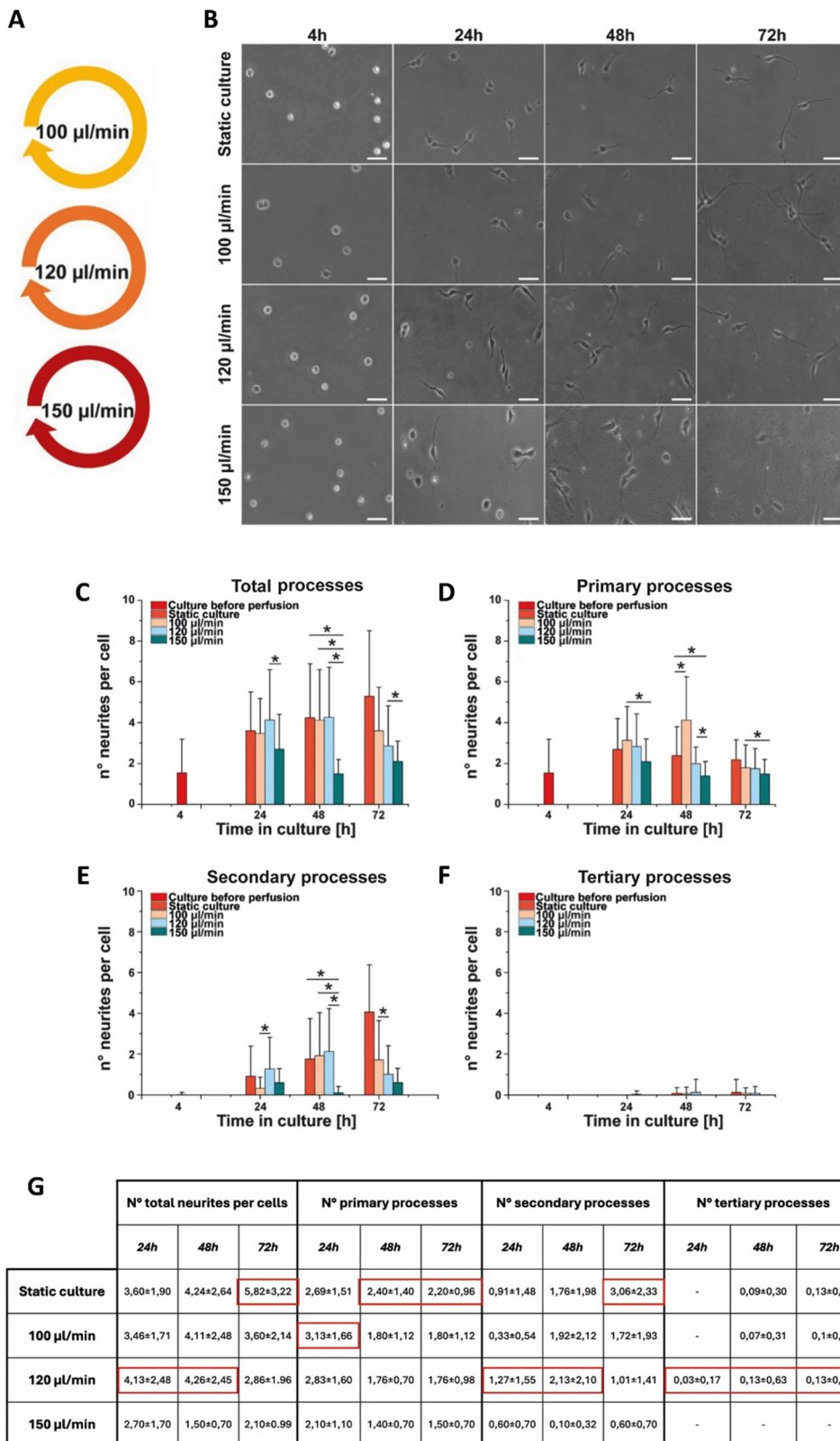


FIG. 1. Stages of neuronal development. (a) Dynamic protocols involving constant flow at 100, 120, and 150 $\mu\text{l}/\text{min}$. (b) Optical images of static and dynamic cultures subjected to constant flow regimes at 100, 120, and 150 $\mu\text{l}/\text{min}$ at 4, 24, 48, and 72 h. Scale bar: 50 μm . (c) Number of total processes, (d) number of primary processes, (e) number of secondary processes, and (f) number of tertiary processes. The morphometric characterization involved the analysis of 100 cells for each condition (*) $p \leq 0.05$ s. (g) Table of the total number of neurites and the number of neurites at different levels of arborization; the red box highlights the best conditions.

reaching 2.86 ± 1.96 neurites per cell at 72 h. Finally, cultures exposed to a flow rate of $150 \mu\text{l}/\text{min}$ after 24 h showed lower values compared to *static* ones, namely, 2.70 ± 1.70 ; this trend was also observed between 48 h and 72 h. In *static cultures*, the number of neurites was found to reach 5.82 ± 3.22 at 72 h, while neurons exposed to $150 \mu\text{l}/\text{min}$ reached a value of 2.10 ± 0.99 .

To fully understand the impact of perfusion on the early stages of neuronal development, a further morphometric analysis was carried out based on the classification in primary, secondary, and tertiary processes. With respect to the effect of constant flow perfusion on primary processes, it was evident that as the flow increased, the number of primary processes decreases over time [Fig. 1(d)]. In *static cultures*, the number of processes did not show any further changing throughout the observation period. After 24 h, the number of primary processes increased in cultures exposed to flow rates of 100 and $120 \mu\text{l}/\text{min}$ compared to *static* cultures. After 48 h, dynamic cultures (100 and $120 \mu\text{l}/\text{min}$) exhibited a decrease in the number of processes compared to the *static* ones (2.40 ± 1.40), reaching then 1.80 ± 1.12 ($100 \mu\text{l}/\text{min}$) and 1.76 ± 0.70 ($120 \mu\text{l}/\text{min}$), respectively, at 72 h, Fig. 1(d). Meanwhile, the number of primary processes in cultures exposed to a constant flow of $150 \mu\text{l}/\text{min}$ decreased from 2.10 ± 1.10 to 1.40 ± 0.70 , reaching 1.50 ± 0.70 at 72 h, Fig. 1(d). Regarding secondary processes, as already known from the literature, they are not expressed until the first 24 h in culture, Fig. 1(e).²⁸ In both *static* and *dynamic* cultures at 100 and $120 \mu\text{l}/\text{min}$, the number of secondary processes increased between 24 and 48 h, with no significant differences, Fig. 1(e). The secondary processes for *dynamic* culture at $150 \mu\text{l}/\text{min}$ did not show significant variation. Specifically, at 48 h, the number of secondary processes for *dynamic* culture at $150 \mu\text{l}/\text{min}$ (0.10 ± 0.31) was significantly lower than the other conditions. At 72 h, the number of secondary processes increased under *static* conditions (3.06 ± 2.33), whereas under *dynamic* ones, it decreased. However, at $100 \mu\text{l}/\text{min}$ (1.71 ± 1.93), this number was significantly higher respect to $120 \mu\text{l}/\text{min}$ (1.01 ± 1.41), Fig. 1(e). Finally, concerning tertiary processes, as demonstrated by the Dotti model, they were absent until 48 h, Fig. 1(f). From the table shown in Fig. 1(g), it is evident that cells cultured under *dynamic* conditions at a constant flow rate of $100 \mu\text{l}/\text{min}$ exhibited a higher number of total neuritic processes at 24 and 48 h compared to *static* conditions, which only appeared to represent the best conditions at 72 h. Moreover, when evaluating different levels of arborization, cells exposed to constant flow rates of 100 and $120 \mu\text{l}/\text{min}$ displayed the highest number of primary, secondary, and particularly tertiary processes.

Neurites were identified as processes extending beyond $10 \mu\text{m}$ from the neuronal soma. The neurites branching and the average length of primary, secondary, and tertiary processes were evaluated to investigate the effect of perfusion on neurite outgrowth and on the subsequent polarization. The average neurites length in *static* cultures was found to increase over time, Fig. 2(a). A similar growth trend was observed for the *dynamic* culture at $100 \mu\text{l}/\text{min}$ [Fig. 2(b)], while neurons exposed to higher flow rates (120 and $150 \mu\text{l}/\text{min}$) showed a rapid increase during the first 48 h, followed by a slight decrease after 3 days under perfusion, Figs. 2(c) and 2(d). In particular, at 24 h, the average length of primary processes of neurons in *static* cultures [Fig. 2(a)] was found to be $24.52 \pm 11.14 \mu\text{m}$, while neurons at $100 \mu\text{l}/\text{min}$ [Fig. 2(b)] showed primary processes shorter than the control ones ($18.46 \pm 9.02 \mu\text{m}$). At 48 h, the average length of primary processes in

static culture and at $100 \mu\text{l}/\text{min}$ was found to be similar. At 72 h, primary processes reached an average length of $59.52 \pm 25.16 \mu\text{m}$ in *static* culture and $46.52 \pm 22.08 \mu\text{m}$ in cultures at $100 \mu\text{l}/\text{min}$. Meanwhile, the results showed that the average length of primary processes exposed to higher flow rates (120 and $150 \mu\text{l}/\text{min}$) rapidly increased during the first 48 h, reaching $49.91 \pm 26.74 \mu\text{m}$ and $51.01 \pm 20.37 \mu\text{m}$, respectively. After that, a slightly decrease was observed in both conditions, reaching $48.42 \pm 25.27 \mu\text{m}$ ($120 \mu\text{l}/\text{min}$) and $44.9 \pm 16.94 \mu\text{m}$ ($150 \mu\text{l}/\text{min}$) at 72 h. The average length of secondary processes was found to be similar in all conditions at 24 h and 48 h, while at 72 h in *static* and *dynamic* cultures (100 and $120 \mu\text{l}/\text{min}$), the average length was found to be $15.71 \pm 10.17 \mu\text{m}$, $9.21 \pm 8.44 \mu\text{m}$, and $6.05 \pm 10.04 \mu\text{m}$, respectively. In *dynamic* cultures at $150 \mu\text{l}/\text{min}$, the average length of secondary processes showed a rapid increase from 1.5 to $7.5 \mu\text{m}$, between 48 and 72 h. Finally, the average length of tertiary processes was found to be comparable in all conditions and with no significant increase observed over time. Moreover, the average growth rate of the major neurite was determined. From the table in Fig. 2(e), it is possible to observe that the average growth rate of the major process was found to be similar between 4 and 24 h in *static* conditions and in the cultures exposed to the highest flow rate ($150 \mu\text{l}/\text{min}$). Otherwise, the major process at 100 and $120 \mu\text{l}/\text{min}$ showed a similar elongation. After that, the average growth rate of the major process increased between 24 and 48 h in all *dynamic* cultures. Specifically, the average growth rates at 100 , 120 , and $150 \mu\text{l}/\text{min}$ were found to be 0.62 , 1.30 , and $0.70 \mu\text{m}/\text{h}$, respectively. Meanwhile, in *static* cultures, a slowdown in the growth rate was observed, with an average value of $0.44 \mu\text{m}/\text{h}$. Between 48 and 72 h, the average growth rate of the major process showed an increase in *static* cultures up to $0.86 \mu\text{m}/\text{h}$. However, in *dynamic* cultures at $100 \mu\text{l}/\text{min}$, the average growth rate decreased 0.53 , whereas for those exposed at 120 and $150 \mu\text{l}/\text{min}$, a retraction was observed, -0.19 and $-0.25 \mu\text{m}/\text{h}$, respectively. These results indicated no particular increase in the growth rate in *dynamic* culture. Moreover, higher flow rates determined a decrease in axonal growth compared to lower flow rates or *static* conditions, confirming thus the results reported before. For these reasons, *variable flow rates* were tested, selecting the flows that provided the best data at different timepoints.

Morphometric characterization under variable flow

Cells exposed to *variable flows* [protocol 1 and protocol 2, Fig. 3(a)] followed the stages of the Dotti model, and this behavior was observed to be similar between *static* and *dynamic* cultures [Fig. 3(b)]. Specifically, the number of neurites per cell showed a continuous increase throughout the culture period in both conditions. After 4 h from plating, the number of total neuritic processes was 2.77 ± 1.62 [Fig. 3(c)]; as shown in Fig. 3(d), these processes correspond to primary ones. Instead, secondary and tertiary processes were completely absent [Figs. 3(e) and 3(f)]. After 24 h, the number of processes per cell under *static* cultures was lower than that under protocol 1 (*static* = 3.23 ± 1.81 vs protocol 1 = 4.86 ± 2.48) and slightly higher than that under protocol 2 (2.71 ± 1.40). This trend was also confirmed by the analysis of the different classes of processes. Specifically, after 24 h under *static* culture, the number of primary processes was found to be 2.28 ± 1.32 [Fig. 3(d)], while they were found to be 3.51 ± 1.77 under protocol 1 and 1.97 ± 1.17 under protocol 2. Related to secondary processes, after 24 h, a slight increase was observed under protocol 1

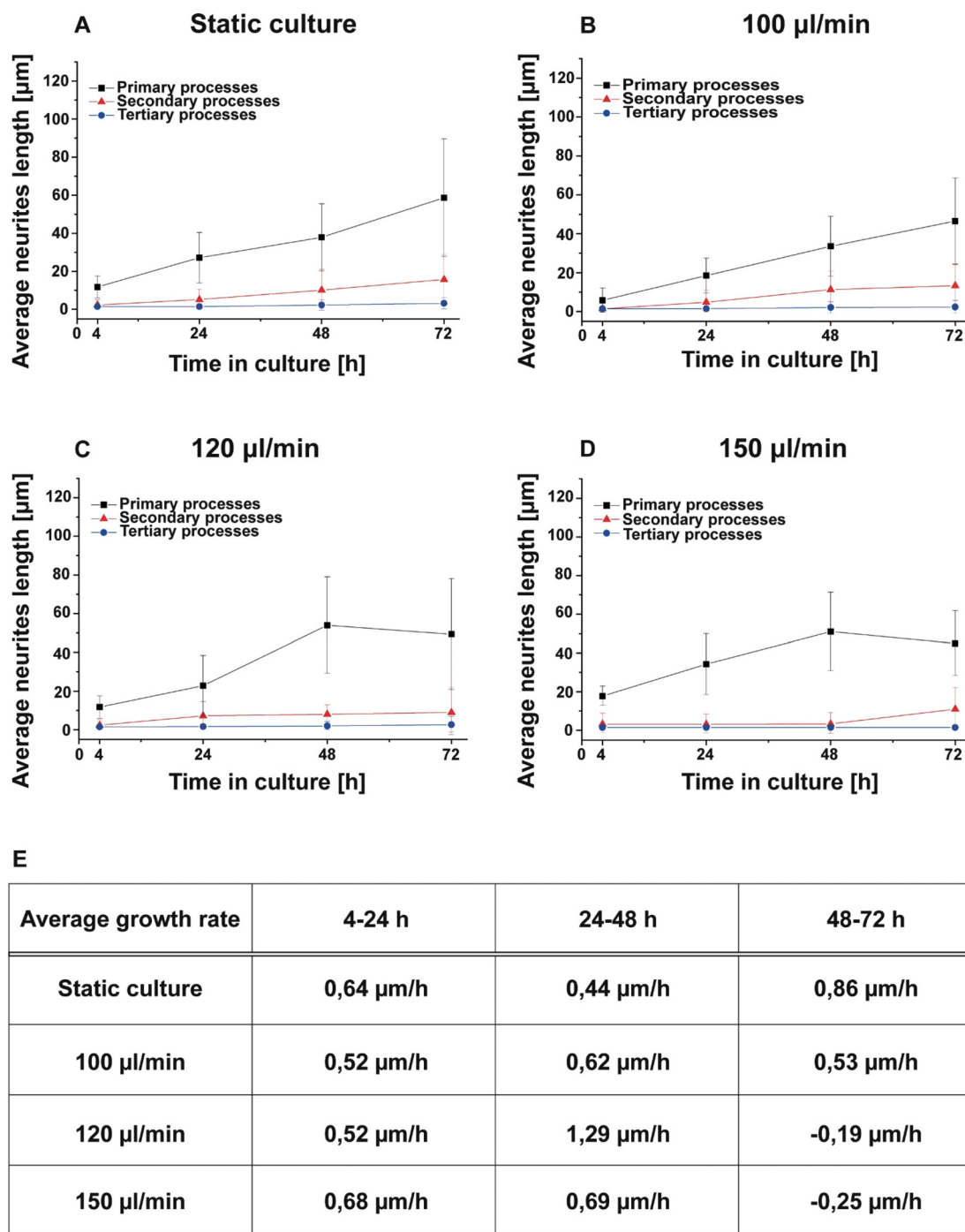


FIG. 2. Morphometric characterization. Average length of primary, secondary, and tertiary processes under *static* (a) and *constant flow regimes* at 100 $\mu\text{l}/\text{min}$ (b), 120 $\mu\text{l}/\text{min}$ (c), 150 $\mu\text{l}/\text{min}$ (d) at 4, 24, 48, 72 h. (e) Table of average growth rate of major neurites expressed in $\mu\text{m}/\text{h}$. The morphometric characterization involved the analysis of 100 cells for each condition.

(1.28 ± 1.56), while under *static cultures* and under *protocol 2*, a similar development was observed (0.91 ± 1.22 and 0.71 ± 1.04 , respectively). Finally, tertiary processes growth only in cultures exposed to *protocol 1*. After 48 h, the number of total processes per cell was

statistically higher in *static cultures* (6.54 ± 1.81) compared to the dynamic ones under both protocols (*protocol 1* = 2.82 ± 1.31 and *protocol 2* = 3.48 ± 1.53). Specifically, as illustrated in Fig. 3(d), the number of primary processes remained quite similar to the ones at 24 h.

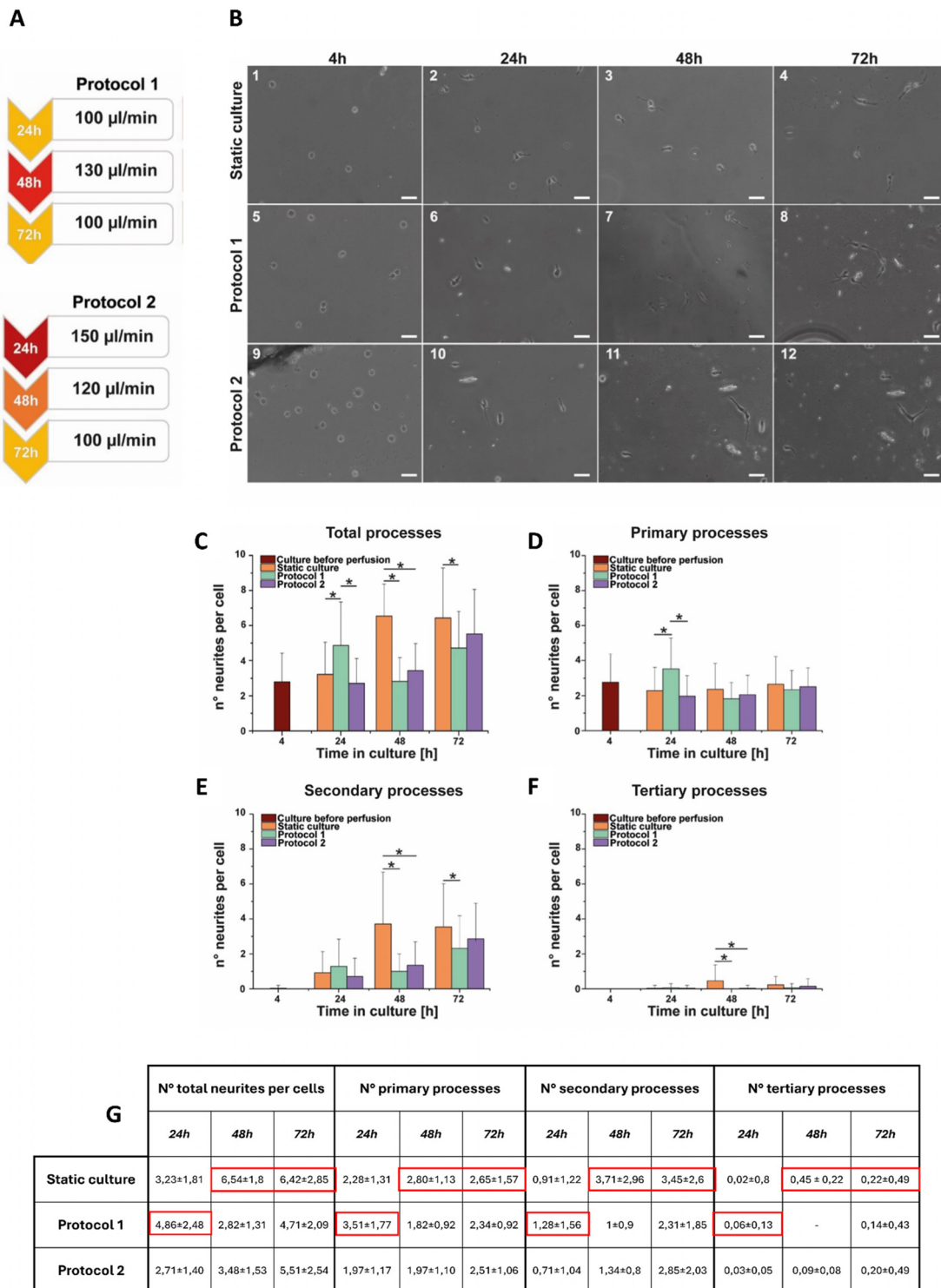


FIG. 3. Stages of neuronal development. (a) Dynamic protocols based on variable flow during the days in culture. (b) Optical images of static cultures and dynamic cultures subjected to variable flow regimes with *protocol 1* and *protocol 2*, at 4, 24, 48, and 72 h. Scale bar: 50 μm . (c) Number of processes, (d) number of primary processes, (e) number of secondary processes, and (f) number of tertiary processes. The morphometric characterization involved the analysis of 100 cells for each condition (*) $p \leq 0.05$. (g) Table of the total number of neurites and the number of neurites at different levels of arborization; the red box highlights the best conditions.

In *static cultures*, it was 2.28 ± 1.13 , while in cultures under *protocol 2*, it was 1.97 ± 1.10 . However, there was a reduction in the number of primary processes under *protocol 1* (1.82 ± 0.92). On the contrary, after 48 h in culture, a substantial increase in the number of secondary processes was observed under *static cultures* (3.71 ± 2.96), while under both dynamic protocols, the values remained relatively similar to those at 24 h, 1 ± 0.9 and 1.34 ± 0.8 , respectively. Moreover, tertiary processes were only observed under *static cultures*, Fig. 3(f). The number of neurites under *static culture* did not show any further changing between 48 and 72 [Fig. 3(c)] reaching 6.42 ± 2.85 neurites per cell at 72 h; specifically, primary processes were found to be 2.65 ± 1.57 [Fig. 3(d)], secondary processes were 3.45 ± 2.46 [Fig. 3(e)], and tertiary processes 0.22 ± 0.49 [Fig. 3(f)]. For cultures under the *dynamic protocols*, the number of processes per cell increased [Fig. 3(c)] reaching 4.71 ± 2.09 under *protocol 1* and 5.51 ± 2.54 under *protocol 2*. In terms of primary processes, the results at 72 h did not show any statistical difference between *static* and *dynamic cultures* (*static* = 2.65 ± 1.57 , *protocol 1* = 2.34 ± 0.92 , and *protocol 2* = 2.51 ± 1.06), Fig. 3(d). Instead, regarding secondary processes, a statistical difference was observed between *static cultures* (3.54 ± 2.46) and *protocol 1* (2.31 ± 1.85), while no significant difference was observed for cultures exposed to *protocol 2* (2.85 ± 2.03), Fig. 3(e). Similar development was observed for tertiary processes. *Protocol 2* exhibited values like the *static* ones, reaching 0.14 ± 0.43 and 0.22 ± 0.49 , respectively. Meanwhile, as it is shown in Fig. 3(f), the number of

tertiary processes was negligible under *protocol 1*. From the table shown in Fig. 3(g), it is evident that cells cultured under *protocol 1* exhibited a higher number of processes per cell during the first 24 h compared to *static cultures*. After this period, the number of processes in cells from *static cultures* was slightly higher than those under *protocol 1*. Meanwhile, cells cultured under *protocol 2* showed the lowest values compared to the other conditions.

The characterization of the average lengths of primary, secondary, and tertiary neuritic processes was carried out on 2D cultures exposed to *protocols 1* and *2* as well. The results obtained from *static cultures*, as described in the previous section ("*Morphometric characterization under constant flow*"), were considered as the control group, Fig. 2(a). The length of neuritic processes was found to increase over time for both *protocols 1* and *2*. Specifically, after 4 h of perfusion, *dynamic cultures* did not show statistically significant differences between the two protocols (*protocol 1*: $18.55 \pm 9.97 \mu\text{m}$ and *protocol 2*: $19 \pm 9.92 \mu\text{m}$), Figs. 4(a) and 4(b). However, in both protocols, the primary processes were slightly longer compared to the control ones ($11.73 \pm 5.70 \mu\text{m}$), Fig. 2(a). Furthermore, the length of primary processes in neurons under *protocol 1* increased more prominently over time compared to the ones under *protocol 2*. Specifically, the length of primary processes under *protocol 1* between 24 and 48 h increased from $42.47 \pm 26.51 \mu\text{m}$ to $67.51 \pm 26.51 \mu\text{m}$, reaching values of $85.46 \pm 38.12 \mu\text{m}$ at 72 h, Fig. 4(a). On the other hand, primary processes in neurons under *protocol 2* showed a slightly increase from

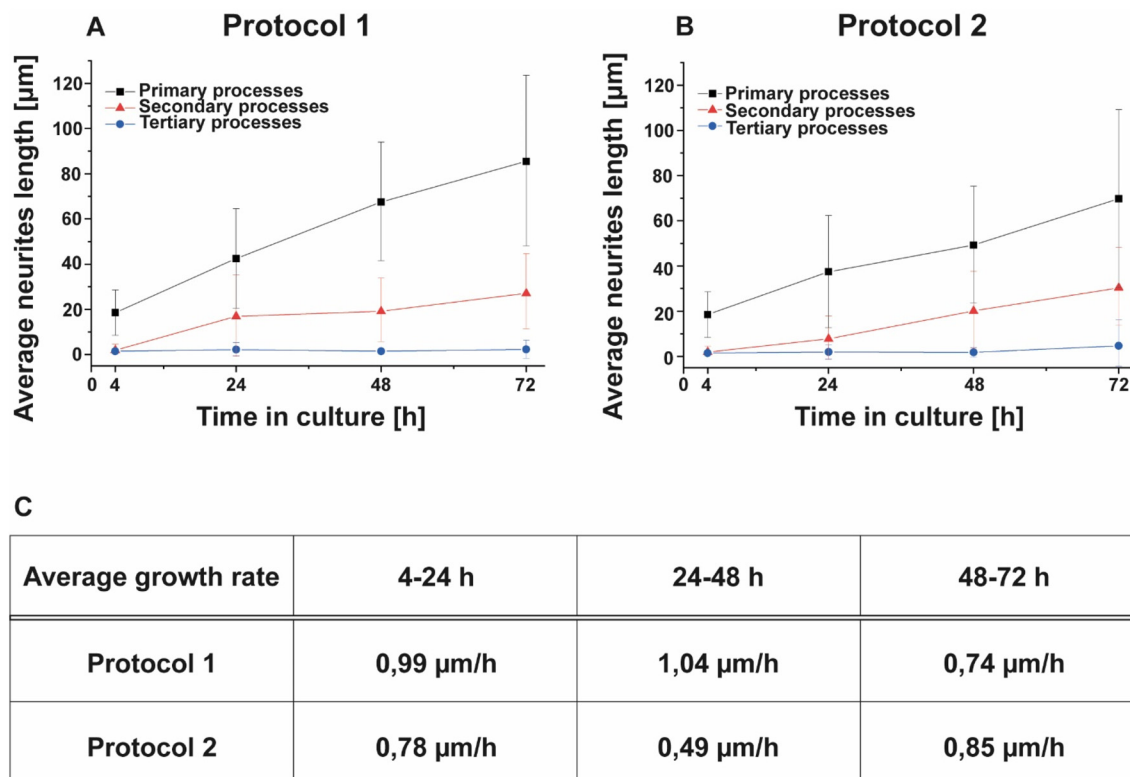


FIG. 4. Morphometric characterization. Average length of primary, secondary, and tertiary processes under and variable flow regimes according to *protocol 1* (a) and *protocol 2* (b) at 4, 24, 48, and 72 h. (c) Table of average growth rate of major neurites expressed in $\mu\text{m}/\text{h}$. The morphometric characterization involved the analysis of 100 cells for each condition.

$37.41 \pm 24.88 \mu\text{m}$ (24 h) to $49.24 \pm 26.03 \mu\text{m}$ (48 h) reaching $69.02 \pm 30.33 \mu\text{m}$ at 72 h, Fig. 4(b). Both dynamic cultures demonstrated higher values compared to static ones, as shown in Fig. 4(a). Related to secondary processes, the results showed that in cultures under *protocol 1*, there was a significant extension in the first 24 h ($12.03 \pm 14.36 \mu\text{m}$), followed by a slowdown in development in the subsequent hours, with values reaching $19.93 \pm 13.63 \mu\text{m}$ at 72 hours, Fig. 4(a). In contrast, cultures exposed to *protocol 2* exhibited a more gradual growth in the first 24 h of perfusion ($4.92 \pm 7.80 \mu\text{m}$), followed by a faster increase between 48 and 72 h, from 13.79 ± 11.37 to $19.93 \pm 13.63 \mu\text{m}$, Fig. 4(b). Again, both protocols supported a higher development of secondary processes compared to *static cultures*, as report in Fig. 2(a). As related to the quantification of the tertiary processes, this task in the first 48 h of culture was challenging due to the fact that these processes at this time are at the very beginning of their development.^{29,30} Nonetheless, the results at 72 h showed that tertiary processes were longer under *protocol 2* than those under *protocol 1*, Figs. 4(a) and 4(b). Finally, the average growth rate of the major neurite was determined. From the table presented in Fig. 4(c), it is evident that the average growth rate of the major processes in cultures under *protocol 1*, between 4 and 24 h, was slightly higher than the ones under *protocol 2*. After that, between 24 and 48 h, the average growth rates of major neurites under *protocol 1* were more than twice higher than the ones under *protocol 2* and under *static conditions*, Fig. 2(e). Moreover, between 48 and 72 h, the average growth rate of major neurites under *protocol 1* was found to be slightly lower than that under *protocol 2* and under *static conditions*, Fig. 2(e).

Morphological evaluation of 2D cell culture

To further evaluate the effect of perfusion on the early-stage development, immunofluorescence characterization was carried out on both *constant* and *variable regime flows*, on three independent cultures for each condition. *Static cultures* were used as control. As a first step, after 7 days, neuronal cultures under *constant flows* were fixed and labeled by β -tubulin III and DAPI. As it can be observed in Fig. 5(a), neuronal morphologies in *static culture* revealed a healthy development, with distinct major and minor neurites, consistent with the data provided by Banker.^{28,29} *Dynamic cultures* under a *constant flow* of $100 \mu\text{l}/\text{min}$ showed neurons still immature, without any neuritic elongation. In contrast, cultures exposed to higher constant flows, 120 and $150 \mu\text{l}/\text{min}$, showed a neuronal development positively affected by flows. Namely, neurons grew and developed a dense network that appears to follow the laminar flow direction.³¹ The immunofluorescence characterization was also carried out onto iNeurons co-cultured with the astrocyte glial fraction under both *protocol 1* and *protocol 2* to assess the morphology of cells exposed to *variable regimes* of flow rates. Cells under *protocol 1* showed the formation of a 2D neuronal network, as already observed under *static conditions*, and neuronal and glial morphologies revealed no differences for both conditions, Fig. 5(b) and *supplementary material*, Fig. 1. In contrast, *protocol 2* was not able to sustain the growth and development of cells over 3 weeks, with the failed formation of a stable network, Fig. 5(b). Based on the morphological results, the synaptic count was performed on both *static cultures* and 2D neuronal networks under *protocol 1*.

The identification of structurally intact excitatory synapse markers was carried out by PSD-95 immunostaining, a postsynaptic scaffolding protein [Fig. 5(c), *supplementary material*, Fig. 2] to

evaluate the effect of perfusion on synaptogenesis and consequently on the development of a functional network. PSD-95 shapes a framework of multiple proteins at excitatory synapses³² that organizes signal transduction and is central to glutamatergic synaptic signaling.³³ Based on the results obtained from the morphometric analysis, the *dynamic cultures* were exposed to a *variable flow* following *protocol 1* up to 25 days. The obtained results showed differences between static and dynamic cultures [Fig. 5(d)], namely, under *static culture*, neurons showed 53 ± 40 PSD-95 puncta/ $100 \mu\text{m}$, while under *dynamic culture*, a PSD-95 puncta density of 88 ± 50 PSD-95 puncta/ $100 \mu\text{m}$ was reached. The results obtained for static cultures were perfectly in line with the ones found in the literature regarding neurons in the second and third layers of the cortex.^{10–12}

Morphological evaluation of 3D cell culture

A preliminary study on the effect of dynamic culture conditions on cell distribution and network development in 3D was carried out by immunostaining and confocal microscopy. Specifically, iNeurons, from healthy donor and primary astrocytes embedded in *NeuroGlycoGel*, were fixed and immunolabeled by β -tubulin III (neurons) and GFAP (astrocytes) after 28 days in culture. Confocal images of 3D cultures under dynamic regimes showed that both cell populations were uniformly distributed within the hydrogel. Namely, neuronal (green) and glial networks (red) were densely developed throughout the 3D structure in both static and dynamic cultures, Fig. 6(a). No apparently differences were observed between the two cultures since the 3D networks developed under *protocol 1* were comparable to those in *static culture*. The same characterization was also performed on a pathological cell line, specifically the human neuroblastoma cells SH-SY5Y, which display catecholaminergic neuronal properties and are commonly used as a model of Parkinson's disease (PD). SH-SY5Y were cultured in *NeuroGlycoGel* and exposed to dynamic conditions following *protocol 1*. *Static cultures* were used as control as well. SH-SY5Y cells were differentiated into the neuronal phenotype between 0 and 10 DIV using retinoic acid and brain-derived neurotrophic factor. In both *static* and *dynamic conditions*, cells were well differentiated with few and short neurites, as expected; moreover, immunostaining of α -synuclein (red) revealed that this protein was significantly evident in both conditions, Fig. 6(b).

DISCUSSION

The advancement of *in vitro* models for the central nervous system (CNS) is rapidly evolving, offering the opportunity to investigate both physiological and pathological brain conditions, significantly contributing to enhance the precision of preclinical research.⁵ It is nowadays recognized that more elaborate designs are needed to accurately recapitulate human physiology/pathophysiology;^{5–7,23} 2D *in vitro* models provide an overly simplified representation of the human body's responses, while animal models often do not adequately represent human conditions. In this respect, indeed 3D culture systems have demonstrated the ability to better replicate tissue architecture and complexity, particularly in terms of cell–ECM interactions and cell–cell communication.³⁴ To better mimic the *in vivo* conditions, bioreactors have gained increasing significance in recent decades due to their ability to regulate the biological and physical conditions of cell and tissue cultures at both macro and, more recently, micro levels.

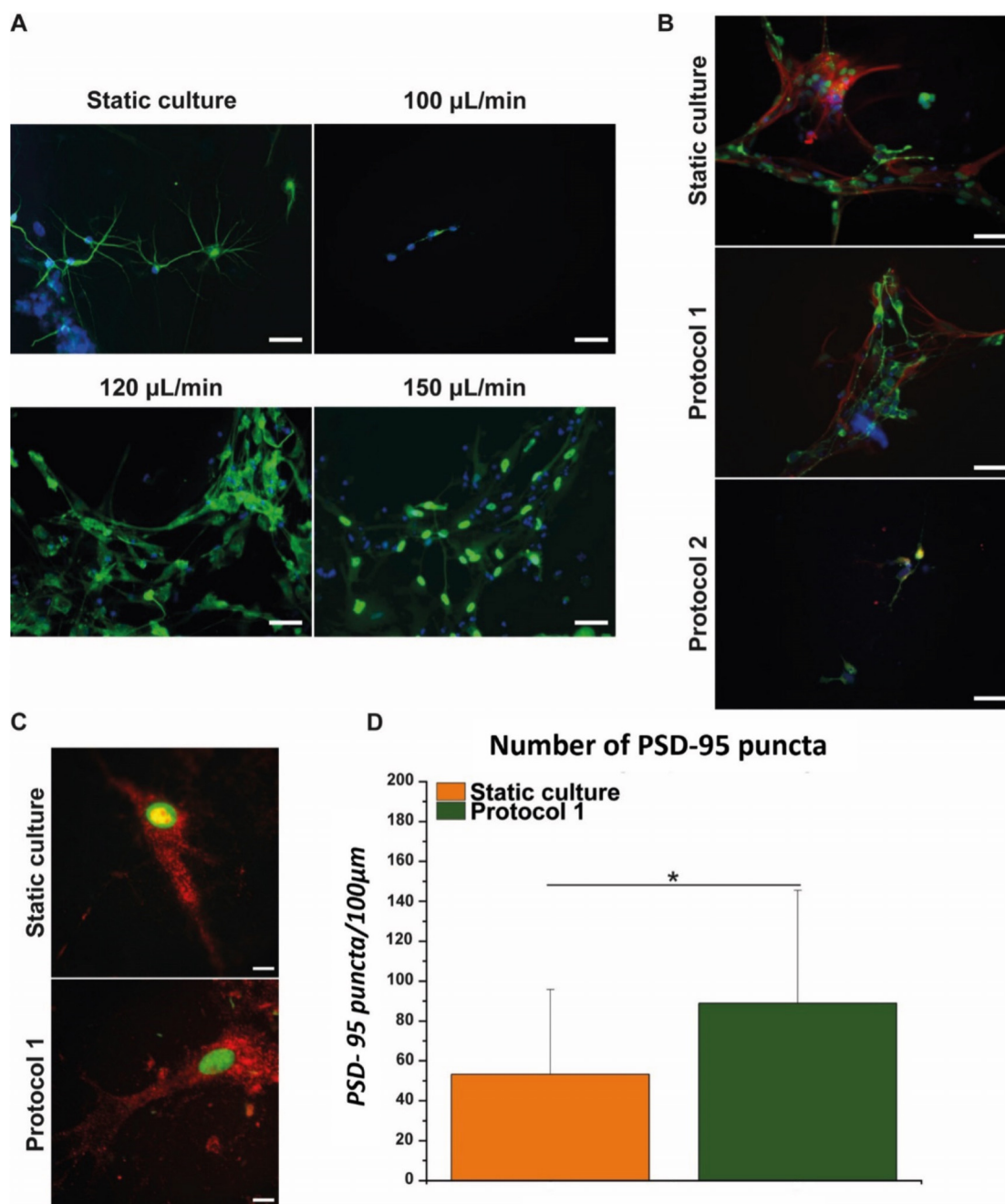


FIG. 5. Optical images of 2D neuronal cultures. (a) 2D static cultures and 2D dynamic cultures perfused with constant flows at 100, 120, and 150 $\mu\text{L}/\text{min}$ labeled for β -tubulin III (green), GFAP (red), and DAPI (blue) at DIV 7; scale bar: 50 μm . Static (b) and dynamic cultures perfused with variable flows according to *protocol 1* and *protocol 2* at DIV 21; scale bar: 10 μm . (c) Representative optical images 2D neuronal cultures, labeled for PSD-95 (red) and DAPI (green), at DIV 25. (d) Quantification of PSD-95 puncta in iNeurons in static culture and dynamic culture perfused with *protocol 1*. The PSD-95 puncta quantification involved the analysis of 100 neuritic processes for each condition (*) $p \leq 0.05$.

Bioreactors have proven to be valuable tools for enhancing *in vitro* culture conditions, creating standardized, scalable, and secure systems for tissue growth.¹⁴ Bioreactors replicate the dynamics of the natural body environment by circulating fluids *in vitro*, making them valuable for

testing regenerative therapies under conditions closer to those encountered *in vivo*. Moreover, bioreactors can provide a useful screening tool for the evaluation of various cell types, biomaterials, drugs, or tissue engineered products prior to animal testing. Compared to *static*

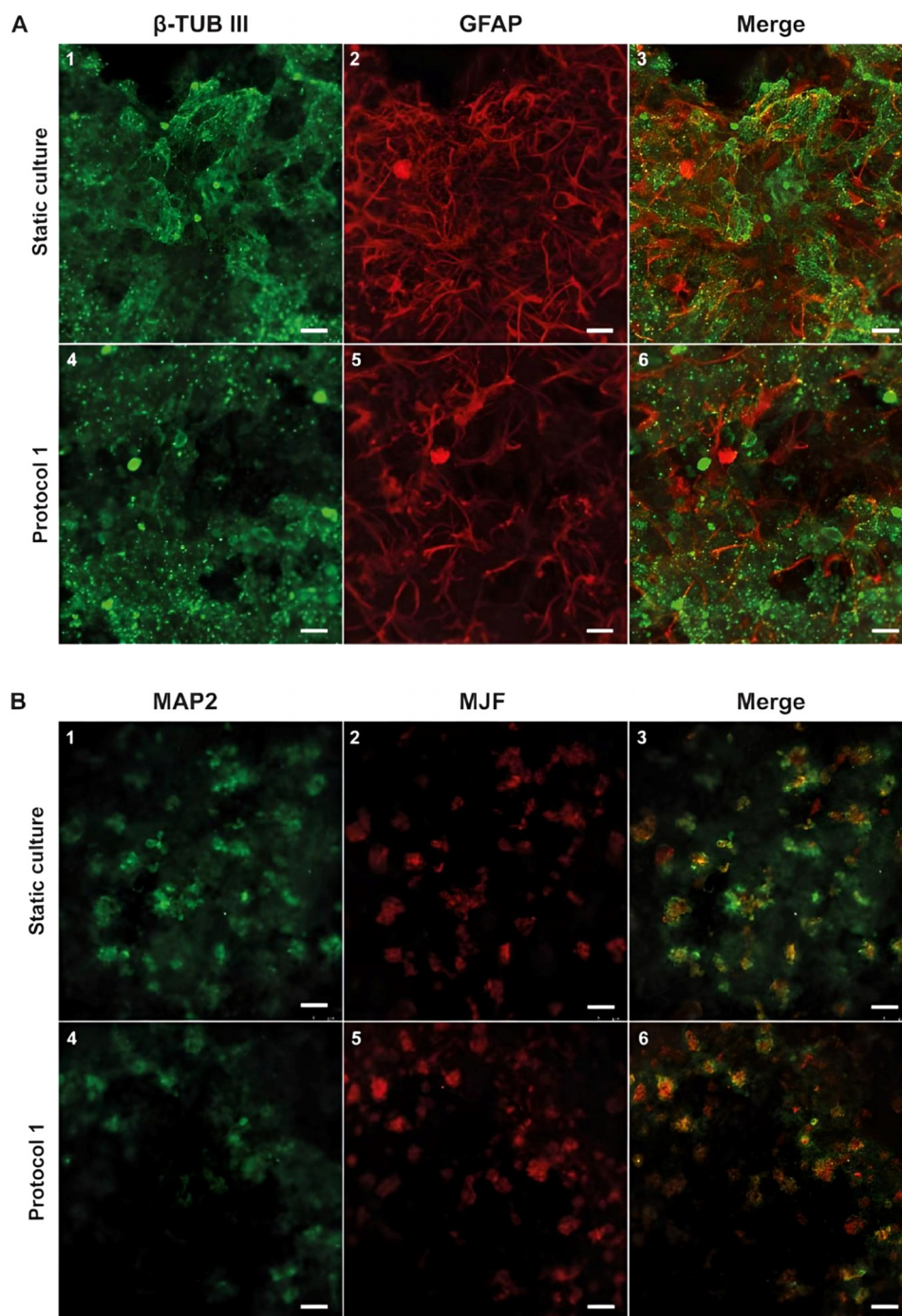


FIG. 6. Morphological characterization of 3D neuronal cultures in both static and dynamic conditions at DIV21. (a) 100 μm z-stack of 3D neuronal culture labeled for β -tubulin III (green) and GFAP (red). (b) 80 μm z-stack of 3D neuroblastoma culture labeled for MAP-2 (green) and MJF (red). Scale bars are 20 μm .

cultures, bioreactors offer higher mass transfer coefficients, which helps reduce the formation of necrotic centers due to oxygen and nutrient deficiencies in the inner layers.²³ While this conventional system may seem straightforward, it remains highly advantageous for modern

applications in neural tissue engineering as well as to model and study acute trauma and degenerative diseases affecting the nervous system. Up to now, bioreactors have been employed to expedite processes and scale up cell cultures, while recent efforts have focused on the

development of devices that replicate the natural microenvironment of the central and peripheral nervous system for *in vitro* experimentation. Culture systems based on *circulating fluids* have effectively demonstrated their ability to facilitate the differentiation of human neural stem cells (hNSCs) from neurospheres into fully developed and functional neurons, astrocytes, and oligodendrocytes;^{20–23} they have also proven capable of accelerating peripheral nerve regeneration and axonal outgrowth within 3D scaffolds.²⁴ For instance, Sun et al. engineered a specialized bioreactor designed to simulate peripheral nerve regeneration within conduits of varying injury gap sizes.³⁵ The study showcased Schwann cell adhesion and alignment along the longitudinal axis of the conduits, closely mimicking natural 3D conditions.^{25,35}

In this work, the use of a commercial bioreactor system, LiveFlow PRO (IVTech S.r.l), has been explored to create a more physiological *in vitro* brain tissue model. We developed and validated a dynamic culture protocol able to sustain both 2D and 3D neuronal cultures based on neurons differentiated from h-iPSCs. Moreover, the dynamic protocol was further characterized with a 3D model based on SH-SY5Y cell line expressed α -synuclein aggregates, aiming to validate it as an alternative platform for studying neurodegenerative diseases like PD. First, the protocol for the 2D cultures under perfusion was optimized by adjusting flow rates to enhance neuronal growth and maturation compared to standard *static cultures*. To evaluate this, the well-established model introduced by Dotti et al. for the polarization process of neurons²⁸ was used. The shape and structure of neurons are crucial for understanding action potential transmission, information processing, and overall neuronal function, while neurite branching influences how individual neurons integrate synaptic inputs^{27,28} and communicate within networks.³¹ Specifically, we assessed both *constant* and *variable flow regimes* because, as documented in the literature, cells exposed to hydrodynamic shear forces develop in response to local changes in fluid velocity.^{31,36} Our findings indicated that different *constant flow* rates had a negligible effect on neuronal development. During the initial 48 h in culture, the number of neuritic processes and branching was enhanced under dynamic conditions, particularly at low flow rates. However, after 72 h, *static cultures* appeared to provide the best conditions. Further analysis revealed that different dynamic culture conditions had variable effects on the length of neuritic processes. High flow rates (120 and 150 $\mu\text{l}/\text{min}$) supported longer neuritic processes during early development, which then attenuated or showed a retroactive behavior at 72 h, while a flow rate of 100 $\mu\text{l}/\text{min}$ provided consistent growth over time. Based on these observations, *variable flow protocols* were developed and characterized to improve dynamic culture conditions. The positive effects of dynamic flow were primarily observed in the average length and average growth rate of neuritic processes rather than in the number of processes and branching. In particular, neurons exposed to both dynamic culture protocols exhibited longer lengths of individual processes at different time points compared to those in *static culture*. This was particularly evident in cultures exposed to *protocol 1*, where, after 24 h in culture, primary, secondary, and tertiary processes showed significantly greater lengths compared to those in *protocol 2* (Fig. 4).

To evaluate neuronal differentiation and 2D networks development under perfusion at *constant flow*, immunostaining for the neuronal marker β -tubulin III was performed. On day 7, the results indicated that extensive neurite outgrowth and long processes were observed only in *dynamic cultures* exposed to high flow rates of 120

and 150 $\mu\text{l}/\text{min}$ [Fig. 5(a)], while *static cultures* and those exposed to lower flow rate (100 $\mu\text{l}/\text{min}$) exhibited few neurons with shorter neuronal processes [Fig. 5(a)]. Under higher flow rates, the spatial organization of neuronal networks appeared to align with the direction of the flow. This directional flow is consistent with the computational model of the bioreactor, where the flow across the cell culture membrane is laminar, free from turbulence or vortices.³⁷ Additionally, to investigate the effect of *variable flows* on the maturation process of neuronal and glial cells, a sequence of immunostaining experiments was carried out. These experiments aimed to highlight the presence of mature neurons and astrocytes, as well as to assess the development of synaptic connections. Double immunostaining for β -tubulin III and GFAP of 4-week-old cultures showed that *protocol 1* sustained the development of 2D co-culture of astrocytes (GFAP) and neurons (β -tubulin III) with extensive neurite outgrowth similar to the *static ones*, while dynamic conditions based on *protocol 2* did not support the network development [Fig. 5(b)]. Based on the morphometric and morphological findings, the synaptic count was performed on both *static cultures* and 2D neuronal networks exposed to *protocol 1*. Neurons under dynamic conditions based on *protocol 1* gave rise to longer neurites and had more abundant synaptic vesicles than those derived under *static conditions*. These findings suggest that, after an initial period of slow neuronal development, the laminar flow microenvironment, provided by *protocol 1*, which maintains consistently low levels of hydrodynamic shear over long-term cultures, offers substantial benefits for the growth and development of neural cells *in vitro*. These results align with observations reported for neural stem cell differentiation in bioreactors.^{38,39}

In conclusion, our results pointed out that neuronal development is favored by dynamic culture conditions with respect to the static ones. The mechanisms underlying this behavior should be characterized in order to fully take advantage of these culture conditions. Indeed, it is nowadays well recognized that mechanical stimulation due to fluid shear forces has an important impact on the reorganization of the cytoskeleton, which in turn controls cell proliferation, migration, and differentiation through different signaling pathways. Moreover, consistent nutrient supply and effective waste removal could contribute to guide neurite outgrowth.¹⁹

Furthermore, a preliminary 3D brain-on-chip model was developed using both human healthy neurons and a human neuroblastoma cell line, often used as the PD model. Neurons derived from h-iPSCs and human neuroblastoma SH-SY5Y cells were encapsulated within *NeuroGlycoGel*, a thermosensitive chitosan-based hydrogel, and exposed to *protocol 1* for 21 days. The effects of perfusion were assessed through morphological characterization using confocal microscopy. In static 3D cultures, cell growth and neural development were sustained although the delivery of nutrients and oxygen to cells may have been limited by the static microenvironment. This positive outcome may be attributed to the well-suited thickness and microporosity of the scaffolds, which supported effective mass transfer. Under dynamic conditions, laminar flow enhanced the growth and development of neural cells without compromising scaffold stability. Specifically, neurons derived from h-iPSCs, co-cultured with astrocytes, showed a homogeneous distribution and the formation of a dense 3D network in both *static* and *dynamic conditions*. No differences in neuronal and glial morphologies were observed between the two conditions. Both neuronal and glial cells showed a typical *in vivo* morphology [Fig. 6(a)], rounding shape for neuronal somata and thin morphology for

astrocytes.^{40–43} These results highlight that the combination of different factors, including physical and chemical cues, substrate stiffness, and 3D arrangement, collectively contributes to supporting an *in vivo*-like growth of the neuronal network.⁴⁴

Finally, a preliminary morphological characterization was carried out on SH-SY5Y cells encapsulated in *NeuroGlycoGel* and exposed to protocol 1. This preliminary characterization aimed to assess the impact of dynamic conditions on neuronal differentiation by comparing the morphology of SH-SY5Y cells treated with RA in *static vs dynamic* 3D cultures. The results obtained through the integration of scaffolds and the bioreactor demonstrated that this system effectively sustained cells growth and differentiation in a dynamic flow environment, Fig. 6(b). Similar observations have been reported in previous studies.^{45,46}

To fully understand the influence of perfusion in 3D neuronal models, further analysis will be essential. Specifically, the influence of perfusion on spontaneous electrophysiological activity should be evaluated also in relation to the presence of an artificial extracellular matrix.^{47,48} These additional studies will help establish this technology as a viable platform for investigating neurodegenerative disorders and conducting pharmacological screening.

CONCLUSION

The use of bioreactors to recreate a more physiologically relevant *in vivo* microenvironment for neuronal differentiation and maturation, both in 2D and 3D configurations, has gained growing interest in the field of neuroengineering. Importantly, the adoption of a perfusion operation mode allows a stable flow of nutrients and differentiation/neurotrophic factors while removing toxic by-products.

In this study, cells in 2D and 3D configurations were exposed to constant and variable fluid flows for up to 28 days in recirculation bioreactors. First, 2D cell cultures demonstrated improvements in cell growth, expression of neural differentiation markers, and neurite morphological development under variable flow regimes compared to static 2D systems. These results indicate that laminar flow at low levels of hydrodynamic shear over long-term culture offers advantages for *in vitro* neural cell growth and network development. Furthermore, a preliminary 3D brain-on-chip model was developed, encapsulating both human neurons and pathological Parkinson's disease (PD) cells, specifically SH-SY5Y cells, within a chitosan-based thermogel. The integration of scaffolds and the bioreactor effectively supported the long-term development of cells and tissues within a dynamic flow environment. Overall, the research aligns with 3R (replacement, reduction, and refinement) principles by proposing alternatives to traditional animal testing. It uses human cells and refines conditions to create more representative and ethically sound preclinical models. This culture system shows promise for generating human 3D neural *in vitro* models, which can serve as valuable tools in preclinical research. They bridge the gap between human clinical studies and animal models, enabling the study of disease onset and progression as well as the preclinical evaluation of new therapeutics and toxicological studies.

METHODS

h-iPSCS and neuronal differentiation

Human induced pluripotent stem cells (h-iPSCs) were generated through lentiviral transduction of fibroblasts obtained from a healthy donor. These cells were generously provided by Frega *et al.* The complete methodology for generating and maintaining the rtTa/NgN2

positive cell line has been previously described.⁴⁹ The differentiation into excitatory cortical layer 2/3 neurons through the overexpression of the neuronal determinant Neurogenin 2 (NgN2) factor started by introducing 4 $\mu\text{g/ml}$ doxycycline (Cat. D5207, Merck Life Science) into Essential 8 Flex Medium (Cat. A2858501, Gibco Thermo Fisher) supplemented with 1% pen-strep, 50 $\mu\text{g/ml}$ of G418 (Cat. G8168, Merck Life Science), and 0.5 $\mu\text{g/ml}$ of puromycin (Cat. P8833, Merck Life Science) defining the step as *Day After Differentiation 0* (DAD 0). On DAD 1, medium was changed using DMEM/F12 supplemented with 1% N2-supplement 100 \times (Cat. 17502048, Gibco, Thermo Fisher), 1% MEM non-essential amino acid solution (Cat. 11140050, Gibco, Thermo Fisher), 1% pen/strep, 10 $\mu\text{g/ml}$ human BDNF, 10 $\mu\text{g/ml}$ human NT-3 (Cat. SRP312, Merck Life Science), and 4 $\mu\text{g/ml}$ doxycycline. At DAD 3, neurons were detached and collected in a 15 ml tube with Neurobasal medium supplemented with 1% pen/strep, 2% B27, 1% glutamax, 10 $\mu\text{g/ml}$ human BDNF, 10 $\mu\text{g/ml}$ human NT-3, and 4 $\mu\text{g/ml}$ doxycycline (*Neurobasal-iN*). After centrifugation (1200 rpm, 5 min), cells were resuspended in 2 ml *Neurobasal-iN*.

Astrocytes

Astrocytes were obtained by brain cortices collected from E18 Sprague-Dawley rat embryos.^{50,51} Astrocytes were cultured in T-75 flasks containing DMEM High Glucose (Cat. 41965039, Gibco, Thermo Fisher), supplemented with 10% FBS and 1% pen/strep. The flasks were placed in incubator at 37 °C with a 5% CO₂ atmosphere, and the culture medium was refreshed every 3 days.

SH-SY5Y

Human neuroblastoma SH-SY5Y cells were cultured in T75 flasks in incubator at 37 °C with 5.5% CO₂. Cells were kindly provided by Schapira's Lab. SH-SY5Y cells were grown in *neuroblastoma medium* based on DMEM/F12 (Cat. 11320074, Gibco, Thermo Fisher) supplemented with 10% fetal bovine serum (FBS, Cat. 10270106, Gibco Invitrogen), 1% penicillin-streptomycin (*pen-strep*, Cat. 15140122, Gibco, Thermo Fisher), and 1% glutamax (Cat. 35050038, Gibco, Thermo Fisher). For the neuronal differentiation, cells were exposed to Neurobasal media (Cat. 21103049, Gibco, Thermo Fisher) supplemented with 1% B27 (Cat. 17504044, Gibco, Thermo Fisher), 1% glutamax, 1% pen-strep, 10 $\mu\text{g/ml}$ human BDNF (Cat. PHC7074, Gibco, Thermo Fisher), and 10 μM all-trans-retinoic acid (RA, Cat. 554720, Merck Life Science) for 10 days (*Neurobasal-SH*); after that, samples were exposed to *Neurobasal-SH* without RA until DIV21.

2D cell culture

The day before plating, cover glasses were functionalized by 1% w/v chitosan solution as reported in the literature.⁵² Chitosan (low molecular weight, 88.3% DDA, lot 281219, from ChitoLytic) 1% (w/v) was dissolved in 0.1 M acetic acid solution (Cat. 695092, Merck Life Science), then sterilized in autoclave at 120 °C for 20 min. Cover glasses were assembled with donuts-shaped Poly-dimethyl-siloxane (PDMS) structures with external diameters of 22 mm and with two different internal configurations: two microchambers for separate cultures [2-MC, Fig. 7(a)] and 1 microchamber for co-culture [1-MC, Fig. 7(b)], and both configurations had an internal diameter of 5 mm. Cover glasses (assembled as explained above) were sterilized in the oven at 120 °C for 2 h. At the end of the

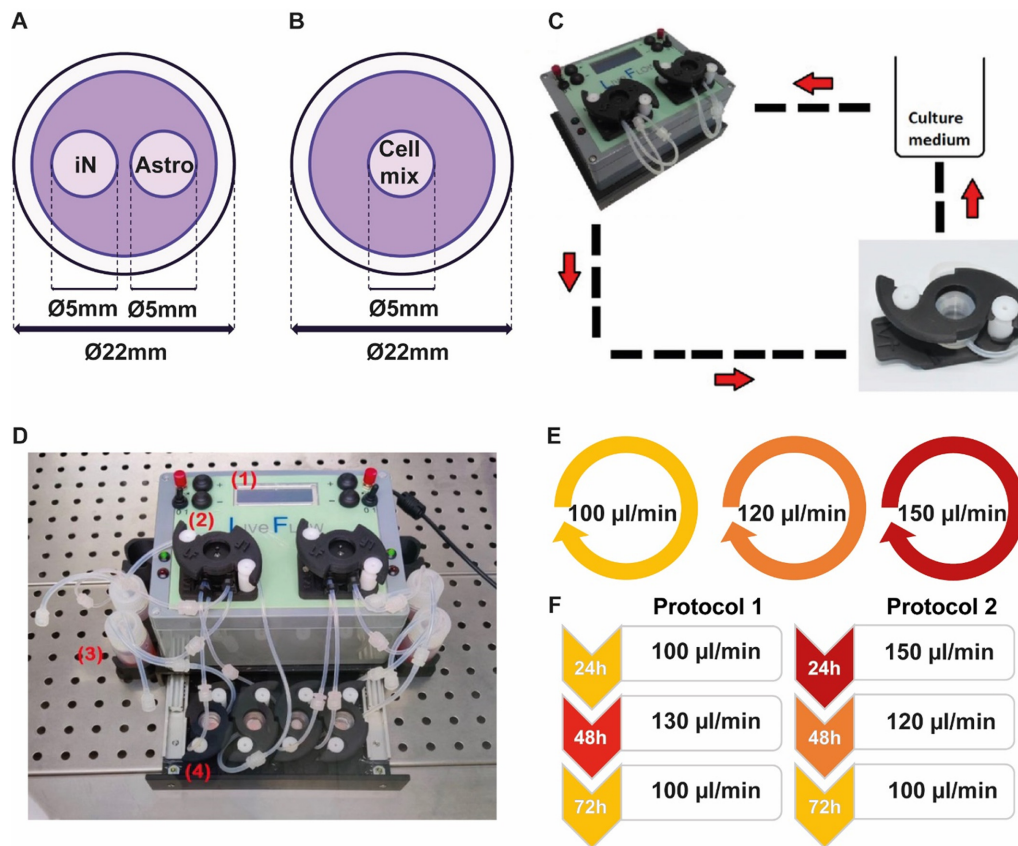


FIG. 7. The IVTech system settings and cell culture protocols. (a)–(b) Cell culture setup: (a) 2-MC configuration for separate culture and (b) 1-MC configuration for co-culture. (c) The fluidic pathway: the peristaltic pump establishes connections with the reservoir and the LB1 bioreactor via silicone tubes. This enables the culture medium to flow through the tubing within the bioreactor, establishing a self-contained fluidic loop. (d) Example of basic system with four LB1: (1) LiveFlow, (2) pumping heads, (3) reservoir for culture medium, and (4) LB1 bioreactor. (e) Dynamic protocols involving constant flow at 100, 120, and 150 µl/min. (f) Dynamic protocols based on variable flow during the days in culture.

sterilization process, the culture supports were treated only on the area delimited by the PDMS structure, with 1% w/v chitosan solution and left in the incubator overnight at 37 °C. The coating solution was removed from the cover glasses, which was then washed twice with water and left to dry under the laminar hood until the plating took place. For neurite outgrowth evaluation, 2-MC configuration was used to plate neurons and astrocytes separately. Specifically, astrocytes were plated at a cell density of 1500 cells/mm² while neurons at 28–30 cells/mm². For morphological characterization and synaptic count, the neuronal and glial (ratio 1:1) co-culture was plated onto 1-MC configuration with a cell density of 1000 and 260–300 cells/mm², respectively. After plating, the samples were incubated in a 37 °C, 5% CO₂ incubator for 4 h to ensure proper cell adhesion.

3D cell culture

NeuroGlycoGel (Bio3Dmatrix Srl, Italy), a thermosensitive hydrogel, was used to encapsulate cells in 3D. *NeuroGlycoGel* consists of two main components: component A, which is the polymeric matrix based on chitosan, and component B, which is the cross-linking solution. Both components are provided in powder form. For preparation, component A is

dissolved in a 0.1 M acetic acid solution, while component B is dissolved in a culture medium. Component A has been autoclaved at 120 °C for 20 min, and component B was filtered using a 0.22 µm syringe filter. *NeuroGlycoGel* was prepared by slowly adding component B drop by drop to component A. To prevent premature or complete gelation, these two components are mixed for 15 min at a temperature of 4 °C. The resultant mixture is then stored in fridge until use. iNeurons, co-cultured with astrocytes (ratio 1:1), and SH-SY5Y cells were suspended and mixed using a positive-displacement pipette directly in *NeuroGlycoGel* solution. Neuroblastoma 3D cultures were obtained with a cell density of 6 × 10⁶ cells/ml. iNeurons 3D cell cultures were obtained with a cell density of 14 × 10⁶ cells/ml. Then, 30 µl of cells/*NeuroGlycoGel* solution mix was poured into a PDMS mold (internal diameter: 5 mm and external diameter: 22 mm) previously placed onto cover glass. All the samples were placed in incubator at 37 °C for 35 min to ensure complete gelation before the addition of culture medium.

IVTech LiveFlow¹ and LiveBox¹

The bioreactor used is the LiveFlow PRO (IVTech s.r.l.). This setup consists of the LiveFlow control unit and the LiveBox1 (LB1)

culture chamber [Fig. 7(c)]. The system is designed to replicate the typical volume of a single well in a 24-well plate. The bioreactor is equipped with two automated peristaltic pumps that work independently, enabling flow rates ranging from 100 to 500 $\mu\text{l}/\text{min}$. Flow rates below 500 $\mu\text{l}/\text{min}$ lead to shear stress levels of 10^{-5} Pa or less at the cell culture surface. These levels represent physiological shear stress, which has been extensively documented in the literature as not impacting cell viability, representing physiological shear stress levels not affecting cell viability as well documented in the literature.^{31,36} Each culture chamber has a wet volume of 1.5 ml and is equipped with both an inlet and an outlet for introducing and removing cell culture media [Fig. 7(d)]. The chamber incorporates a Luer-locking system, ensuring a tight seal of the system under both static and dynamic conditions (up to 1 ml/min). Samples, specifically arranged on circular cover glasses ($\text{Ø}22$ mm), can be placed in the bioreactor chamber. A S-shape clamp fixation system guarantees an airtight seal for all components. The culture medium flow within the chamber is characterized as laminar and tangential to the culture contained within it.³¹ All the components of the IVTech bioreactor were autoclaved before experiments.

Considering the maximum limit of 200 $\mu\text{l}/\text{min}$ to ensure laminar flow,^{31,53,54} different constant flow rates were tested on both separated and mixed dynamical cultures: 100, 120, and 150 $\mu\text{l}/\text{min}$. Constant flows were maintained throughout the culture period [Fig. 7(e)].

Variable flows were tested to evaluate the effect of perfusion on neuronal growth and maturation. Specifically, two protocols were developed and tested based on the results obtained from constant flow experiments, selecting the optimal flow rates in terms of average growth rate of neuritic development. In both protocols, the flow rate was modified every 24 h during the first 3 days in culture [Fig. 7(f)]. As related to protocol 1, on day 1 the samples were exposed to a flow of 100 $\mu\text{l}/\text{min}$, on day 2, the flow rate was increased to 130 $\mu\text{l}/\text{min}$, and on day 3, it was brought back to 100 $\mu\text{l}/\text{min}$. As relates to protocol 2, on day 1 the samples were exposed to a flow of 150 $\mu\text{l}/\text{min}$, on day 2, the flow rate was lowered to 120 $\mu\text{l}/\text{min}$, and on day 3, it was further reduced to 100 $\mu\text{l}/\text{min}$. Starting from day 4, a constant flow rate of 100 $\mu\text{l}/\text{min}$ was maintained until the end of culture.

Dynamic 2D cell cultures

For dynamic cultures, both cell culture configurations (1-MC and 2-MC) were prepared and incubated for 4 h before perfusion. All samples were observed 4 h post-plating and then placed inside the LB1. LB1 was filled with 1 ml of culture medium and sealed with clamps. The fluidic circuit was assembled as shown in Fig. 7(d). After filling the circuit with 15 ml of culture medium, the peristaltic pumps were activated at different speeds. Constant and variable flow rates were tested. The culture medium in the reservoir was partially changed every 72 h. The whole setup was placed in incubator at 37 °C, 95% humidity, and 5% CO₂. Moreover, both cell culture configurations were prepared, transferred into a 12-well plate, and placed in incubator at 37 °C, 5% CO₂, and 95% humidity, to be used as static control.

Dynamic 3D cell cultures

3D cultures of both cell populations were placed into LB1. LB1 was filled with 1 ml of culture medium and sealed with clamps. The fluidic circuit was assembled as already explained in Fig. 7(c). After filling the circuit with 15 ml of culture medium, the peristaltic pumps

were activated. Based on preliminary results obtained from the 2D dynamic cultures, protocol 1 was selected as the best dynamic condition able to improve growth and maturity compared to static culture condition without compromising cell viability. For human derived neurons co-culture with astrocytes, *Neurobasal-iN* into the reservoir was partially changed every 72 h. For SH-SY5Y samples, *Neurobasal-SH* was partially changed every 48 h. In parallel, as static control, 3D cultures were transferred into 12-well plates and placed in incubator at 37 °C, 5% CO₂, and 95% humidity.

Morphometric characterization

To assess neuronal development and polarization, a morphometric study was conducted on the 2D model, both in static conditions and under perfusion, using the classification model proposed by Dotti *et al.*^{28,29} Neuronal polarity is defined as neurons developing two distinct types of extensions: axons and dendrites. The model identified five well-defined stages of morphological development. Recently, this model, which is based on the use of poly-lysine and poly-ornithine as adhesion factors, was used to validate chitosan as an alternative adhesion factor for primary and iNeurons cultured under static conditions.⁵² The morphometric characterization was carried out focusing on cells that were not in contact with other cells. The classification involves different stages: stage 1, cells without neurites, stage 2, cells with some neurites lacking axonal markers, indicating no axonal differentiation, stage 3, cells with an axon, stage 4, cells with growing dendrites, and stage 5, mature cells. From the morphometric analysis, the following parameters were extracted:

- the number of neuritic processes;
- the number of primary, secondary, and tertiary processes;
- the length of primary, secondary, and tertiary processes;
- the growth rate of the major process.

Neurites were defined as processes extending over 10 μm from the cell body, with a length of at least one cell body diameter. Furthermore, with respect to the number of neurites and to the average neurites length, extensive analysis was carried out to differentiate neuritic process into primary, secondary, and tertiary ones on the basis of their branching order.⁵⁵ Primary processes are the initial extensions that originate from the cell body, secondary processes branch out from primary ones, and tertiary processes further branch from secondary extensions. Additionally, neuritic processes can give rise to dendritic spines, which establish synaptic connections with other neurons.⁵⁵ All neuritic processes were considered minor except for the longest one, the axon. Major neurites were those with the greatest length compared to other neurites of the cell, being at least 10–20 μm longer. In the experiments, an Olympus IX-51 inverted microscope with a DP70 digital camera and a CPlan 10 N.A. 0.25 PhC objective was used to acquire phase contrast images. For each condition, 100 cells were acquired and analyzed using ImageJ with the NeuronJ plugin for tracing, analyzing, and measuring neuritic processes. All graphs presented in the study were based on data obtained from three separate experiments. Both static and dynamic neuronal cultures were observed at 4, 24, 48, and 72 h after plating.

Immunocytochemistry

Both 2D and 3D cell cultures under static and dynamic conditions were fixed with 4% paraformaldehyde at room temperature for

10 and 30 min, respectively. Cell permeabilization was carried out with Triton X-100 (Cat. X100, Merck Life Science) at 0.1% (2D) and 0.3% (3D) for 10 and 30 min, respectively. Cultures were rinsed three times with phosphate-buffered saline solution (PBS, Cat. 18912014, Gibco, Thermo Fisher) and then were incubated with blocking buffer solution composed of 0.3% bovine serum albumin (Cat. A9418, Merck Life Science) and 0.5% FBS at 4 °C for 45 min (2D) and 2 h (3D) to block nonspecific binding of antibodies. Cultures were exposed to a primary antibody for 90 min (2D) and overnight at 4 °C (3D). Specifically, β -tubulin III (1:200, microtubules, Cat. 60100, Voden medical instruments), MAP-2 (1:500, dendritic microtubule-associated protein, Cat. 188 002 and 188 011, Synaptic System), MJFR-14-6-4-2 (1:250, anti-Alpha-synuclein aggregate antibody, Cat. b138501, abcam), GFAP (1:500, glial fibrillary acidic protein, Cat. 173 002 and 173 01, Synaptic System), PSD-95 (1:200, postsynaptic density, Cat. MA1-046, Invitrogen, Thermo Fisher), and DAPI (1:10000, nuclei, Cat. 75004, Voden medical instruments) were used as primary antibodies. Cultures were exposed to the secondary antibodies: Alexa Fluor 488 and Alexa Fluor 549 Goat anti mouse or Goat anti rabbit (Cat. A11001, A11003, A11008, A11035, Gibco, Thermo Fisher) diluted 1:700 and 1:1000. Postsynaptic density puncta were calculated by SynapCountJ, an ImageJ plugin that counts puncta and returns puncta density value in 100 μm . The analysis was carried out on 100 neuritic processes randomly chosen, with a length of at least 20 μm and considering the process from 10 μm distance from the soma. 2D samples were observed using the Olympus BX51M fluorescence microscope, equipped with the Hamamatsu ORCA-ER C4742-80 digital camera driven by Image ProPlus software (Media Cybernetic). 3D samples were observed by a confocal imaging Leica STELLARIS 8 Falcon τ -STED inverted confocal/STED microscope (Leica Microsystems, Mannheim, Germany).

Statistical analysis

Statistical analysis was carried out using MATLAB (The MathWorks, Natick, MA, USA). The significative differences between experimental and control values were analyzed by the statistical non-parametric Kruskal-Wallis's test, since data do not follow a normal distribution (evaluated by the Kolmogorov-Smirnov normality test). Differences were considered statistically significant when $p < 0.05$ (*).

SUPPLEMENTARY MATERIAL

See the [supplementary material](#) for details of both optical contrast phase and fluorescence images of a 2D neuronal network under *static* and *dynamic conditions*, perfused with variable flows according to *protocol 1* at DIV 25 (Fig. S1) and fluorescence images of synaptic puncta of 2D neuronal cultures at DIV 25 under *static* and *dynamic conditions*, also perfused with variable flows according to *protocol 1* (Fig. S2).

ACKNOWLEDGMENTS

The authors thank CNPH laboratory (University of Twente) for providing hiPSCs rtTa/NgN2 positive line, Marloes R. Levers from CNPH group for teaching stem cell maintaining and differentiation. The authors thank Schapira's Lab for providing SH-SY5Y cells. The authors thank Sara Pepe and Anna Fassio (DIMES, University of Genoa) for providing primary astrocytes. The authors thanks *Dipartimento di Fisica*, University of Genoa, DIFILAB, and Professor Diaspro Alberto research group.

This work was partially supported by the Italian Ministry of Research, under the complementary actions to the NRRP "Fit4MedRob - Fitfor MedicalRobotics" Grant (No. PNC0000007).

AUTHOR DECLARATIONS

Conflict of Interest

The authors have no conflicts to disclose.

Ethics Approval

Ethics approval is not required.

Author Contributions

Donatella Di Lisa: Conceptualization (equal); Data curation (equal); Funding acquisition (equal); Investigation (equal); Methodology (equal); Project administration (equal); Supervision (equal); Validation (equal); Writing – original draft (equal). **Andrea Andolfi:** Conceptualization (equal); Data curation (equal); Investigation (equal); Methodology (equal); Validation (equal); Visualization (equal); Writing – original draft (equal); Writing – review & editing (equal). **Giacomo Masi:** Data curation (equal); Formal analysis (equal); Investigation (equal); Visualization (equal); Writing – review & editing (equal). **Giuseppe Uras:** Data curation (equal); Formal analysis (equal); Investigation (equal); Validation (equal); Writing – review & editing (equal). **Pier Francesco Ferrari:** Validation (equal); Writing – review & editing (equal). **Sergio Martinoia:** Funding acquisition (equal); Writing – review & editing (equal). **Laura Pastorino:** Conceptualization (equal); Funding acquisition (equal); Project administration (equal); Supervision (equal); Writing – original draft (equal); Writing – review & editing (equal).

DATA AVAILABILITY

The data that support the findings of this study are available from the corresponding author upon reasonable request.

REFERENCES

- ¹D. Pacitti, R. Privolizzi, and B. E. Bax, "Organs to cells and cells to organoids: The evolution of in vitro central nervous system modelling," *Front. Cell. Neurosci.* **13**, 129 (2019).
- ²V. K. Gribkoff and L. K. Kaczmarek, "The need for new approaches in CNS drug discovery: Why drugs have failed, and what can be done to improve outcomes," *Neuropharmacology* **120**, 11–19 (2017).
- ³C. Jensen and Y. Teng, "Is it time to start transitioning from 2D to 3D cell culture?," *Front. Mol. Biosci.* **7**, 33 (2020).
- ⁴T. M. Dawson, T. E. Golde, and C. Lagier-Tourenne, "Animal models of neurodegenerative diseases," *Nat. Neurosci.* **21**(10), 1370–1379 (2018).
- ⁵P. Nikolakopoulou, R. Rauti, D. Voulgaris, I. Shlomy, B. M. Maoz, and A. Herland, "Recent progress in translational engineered in vitro models of the central nervous system," *Brain* **143**(11), 3181–3213 (2020).
- ⁶C.-M. Moysidou, C. Barberio, and R. M. Owens, "Advances in engineering human tissue models," *Front. Bioeng. Biotechnol.* **8**, 620962 (2021).
- ⁷S. Afewerki, T. D. Stocco, A. D. R. da Silva, A. S. A. Furtado, G. F. de Sousa, G. U. Ruiz-Esparza, T. J. Webster, F. R. Marciano, M. Strømme, and Y. S. Zhang, "In vitro high-content tissue models to address precision medicine challenges," *Mol. Aspects Med.* **91**, 101108 (2023).
- ⁸P. Srikanth and T. L. Young-Pearse, "Stem cells on the brain: Modeling neurodevelopmental and neurodegenerative diseases using human induced pluripotent stem cells," *J. Neurogenet.* **28**(1–2), 5–29 (2014).

- ⁹Y. J. Hong and J. T. Do, "Neural lineage differentiation from pluripotent stem cells to mimic human brain tissues," *Front. Bioeng. Biotechnol.* **7**, 400 (2019).
- ¹⁰M. L. Lovett, T. J. Nieland, Y. L. Dingle, and D. L. Kaplan, "Innovations in 3D tissue models of human brain physiology and diseases," *Adv. Funct. Mater.* **30**(44), 1909146 (2020).
- ¹¹M. Cadena, L. Ning, A. King, B. Hwang, L. Jin, V. Serpooshan, and S. A. Sloan, "3D bioprinting of neural tissues," *Adv. Healthcare Mater.* **10**(15), 2001600 (2021).
- ¹²H.-Y. Tan, H. Cho, and L. P. Lee, "Human mini-brain models," *Nat. Biomed. Eng.* **5**(1), 11–25 (2020).
- ¹³X. Huang, Z. Huang, W. Gao, W. Gao, R. He, Y. Li, R. Crawford, Y. Zhou, L. Xiao, and Y. Xiao, "Current advances in 3D dynamic cell culture systems," *Gels* **8**(12), 829 (2022).
- ¹⁴N. Sarkar, S. Bhumiratana, L. Geris, I. Papanitiou, and W. L. Grayson, "Bioreactors for engineering patient-specific tissue grafts," *Nat. Rev. Bioeng.* **1**(5), 361–377 (2023).
- ¹⁵C. McKee and G. R. Chaudhry, "Advances and challenges in stem cell culture," *Colloids Surf., B* **159**, 62–77 (2017).
- ¹⁶C. Kropp, D. Massai, and R. Zweigerdt, "Progress and challenges in large-scale expansion of human pluripotent stem cells," *Process Biochem.* **59**, 244–254 (2017).
- ¹⁷L. Miles, J. Powell, C. Kozak, and Y. Song, "Mechanosensitive ion channels, axonal growth, and regeneration," *Neuroscientist* **29**(4), 421–444 (2023).
- ¹⁸V. Raffia, *Force: A Messenger of Axon Outgrowth* (Elsevier, 2023), Vol. 140, pp 3–12.
- ¹⁹E. Babaliari, A. Ranella, and E. Stratakis, "Microfluidic systems for neural cell studies," *Bioengineering* **10**(8), 902 (2023).
- ²⁰C. Selden and B. Fuller, "Role of bioreactor technology in tissue engineering for clinical use and therapeutic target design," *Bioengineering* **5**(2), 32 (2018).
- ²¹S. Ahmed, V. M. Chauhan, A. M. Ghaemmaghami, and J. W. Aylott, "New generation of bioreactors that advance extracellular matrix modelling and tissue engineering," *Biotechnol. Lett.* **41**, 1–25 (2019).
- ²²S. Nemat, S. Abbasalazadeh, and H. Baharvand, "Scalable expansion of human pluripotent stem cell-derived neural progenitors in stirred suspension bioreactor under xeno-free condition," in *Bioreactors in Stem Cell Biology: Methods and Protocols*, edited by K. Turksen (Humana Press, New York, 2016), Vol. 1502, pp. 143–158.
- ²³P. M. Holloway, S. Willaime-Morawek, R. Siow, M. Barber, R. M. Owens, A. D. Sharma, W. Rowan, E. Hill, and M. Zagnoni, "Advances in microfluidic in vitro systems for neurological disease modeling," *J. Neurosci. Res.* **99**(5), 1276–1307 (2021).
- ²⁴R. Habibey, J. E. Rojo Arias, J. Striebel, and V. Busskamp, "Microfluidics for neuronal cell and circuit engineering," *Chem. Rev.* **122**(18), 14842–14880 (2022).
- ²⁵B. Zhang and M. Radisic, "Organ-on-a-chip devices advance to market," *Lab Chip* **17**(14), 2395–2420 (2017).
- ²⁶A. Naderi, N. Bhattacharjee, and A. Folch, "Digital manufacturing for microfluidics," *Annu. Rev. Biomed. Eng.* **21**, 325–364 (2019).
- ²⁷H. Xicoy, B. Wieringa, and G. J. Martens, "The SH-SY5Y cell line in Parkinson's disease research: A systematic review," *Mol. Neurodegener.* **12**, 1–11 (2017).
- ²⁸C. G. Dotti, C. A. Sullivan, and G. A. Banker, "The establishment of polarity by hippocampal neurons in culture," *J. Neurosci.* **8**(4), 1454–1468 (1988).
- ²⁹C. G. Dotti and G. A. Banker, "Experimentally induced alteration in the polarity of developing neurons," *Nature* **330**(6145), 254–256 (1987).
- ³⁰Y. Ohara, N. Koganezawa, H. Yamazaki, R. T. Roppongi, K. Sato, Y. Sekino, and T. Shirao, "Early-stage development of human induced pluripotent stem cell-derived neurons," *J. Neurosci. Res.* **93**(12), 1804–1813 (2015).
- ³¹S. Giusti, D. Mazzei, L. Cacopardo, G. Mattei, C. Domenici, and A. Ahluwalia, "Environmental control in flow bioreactors," *Processes* **5**(2), 16 (2017).
- ³²E. Kim and M. Sheng, "PDZ domain proteins of synapses," *Nat. Rev. Neurosci.* **5**(10), 771–781 (2004).
- ³³L. Ugalde-Triviño and M. Díaz-Guerra, "PSD-95: An effective target for stroke therapy using neuroprotective peptides," *Int. J. Mol. Sci.* **22**(22), 12585 (2021).
- ³⁴R. Rauti, N. Renous, and B. M. Maoz, "Mimicking the brain extracellular matrix in vitro: A review of current methodologies and challenges," *Israel J. Chem.* **60**(12), 1141–1151 (2020).
- ³⁵T. Sun, D. Norton, N. Vickers, S. L. McArthur, S. M. Neil, A. J. Ryan, and J. W. Haycock, "Development of a bioreactor for evaluating novel nerve conduits," *Biotech. Bioeng.* **99**(5), 1250–1260 (2008).
- ³⁶D. Mazzei, M. Guzzardi, S. Giusti, and A. Ahluwalia, "A low shear stress modular bioreactor for connected cell culture under high flow rates," *Biotech. Bioeng.* **106**(1), 127–137 (2010).
- ³⁷L. Cacopardo, J. Costa, S. Giusti, L. Buoncompagni, S. Meucci, A. Corti, G. Mattei, and A. Ahluwalia, "Real-time cellular impedance monitoring and imaging of biological barriers in a dual-flow membrane bioreactor," *Biosens. Bioelectron.* **140**, 111340 (2019).
- ³⁸H. J. Lin, T. J. O'Shaughnessy, J. Kelly, and W. Ma, "Neural stem cell differentiation in a cell–collagen–bioreactor culture system," *Dev. Brain Res.* **153**(2), 163–173 (2004).
- ³⁹S. Gerecht-Nir, S. Cohen, and J. Itskovitz-Eldor, "Bioreactor cultivation enhances the efficiency of human embryoid body (hEB) formation and differentiation," *Biotech. Bioeng.* **86**(5), 493–502 (2004).
- ⁴⁰M. T. Tedesco, D. Di Lisa, P. Massobrio, N. Colistra, M. Pesce, T. Catelani, E. Dellacasa, R. Raiteri, S. Martinoia, and L. Pastorino, "Soft chitosan microbeads scaffold for 3D functional neuronal networks," *Biomaterials* **156**, 159–171 (2018).
- ⁴¹D. K. Cullen, J. A. Wolf, V. N. Vernekar, J. Vukasinovic, and M. C. LaPlaca, "Neural tissue engineering and biohybridized microsystems for neurobiological investigation in vitro (part 1)," *Crit. Rev. Biomed. Eng.* **39**(3), 201 (2011).
- ⁴²A. L. Placone, P. M. McGuiggan, D. E. Bergles, H. Guerrero-Cazares, A. Quiñones-Hinojosa, and P. C. Searson, "Human astrocytes develop physiological morphology and remain quiescent in a novel 3D matrix," *Biomaterials* **42**, 134–143 (2015).
- ⁴³S. Balasubramanian, J. A. Packard, J. B. Leach, and E. M. Powell, "Three-dimensional environment sustains morphological heterogeneity and promotes phenotypic progression during astrocyte development," *Tissue Eng., Part A* **22**(11–12), 885–898 (2016).
- ⁴⁴S. Grossepy, P. P. Chan, and P. M. Doran, "Stimulation of cell growth and neurogenesis using protein-functionalized microfibrous scaffolds and fluid flow in bioreactors," *Biochem. Eng. J.* **159**, 107602 (2020).
- ⁴⁵D. H. Park, M. T. He, E. J. Cho, K. Morten, and J. S. Go, "Development of a novel microfluidic perfusion 3D cell culture system for improved neuronal cell differentiation," *Biomed. Microdev.* **25**(3), 22 (2023).
- ⁴⁶D. Simao, C. Pinto, S. Piersanti, A. Weston, C. J. Peddie, A. E. Bastos, V. Licursi, S. C. Schwarz, L. M. Collinson, and S. Salinas, "Modeling human neural functionality in vitro: Three-dimensional culture for dopaminergic differentiation," *Tissue Eng., Part A* **21**(3–4), 654–668 (2015).
- ⁴⁷C. F. López-León, J. Soriano, and R. Planet, "Rheological characterization of three-dimensional neuronal cultures embedded in PEGylated fibrin hydrogels," *Gels* **9**(8), 642 (2023).
- ⁴⁸C. F. López-León, R. Planet, and J. Soriano, "Preparation and mechanical functional characterization of PEGylated fibrin hydrogels: impact of thrombin concentration," *Gels* **10**(2), 116 (2024).
- ⁴⁹M. Frega, S. H. Van Gestel, K. Linda, J. Van Der Raadt, J. Keller, J.-R. Van Rhijs, D. Schubert, C. A. Albers, and N. N. Kasri, "Rapid neuronal differentiation of induced pluripotent stem cells for measuring network activity on micro-electrode arrays," *JoVE* **119**, e54900 (2017).
- ⁵⁰D. Aprile, F. Fruscione, S. Baldassari, M. Fadda, D. Ferrante, A. Falace, E. Buhler, J. Sartorelli, A. Represa, and P. Baldelli, "TBC1D24 regulates axonal outgrowth and membrane trafficking at the growth cone in rodent and human neurons," *Cell Death Differ.* **26**(11), 2464–2478 (2019).
- ⁵¹E. Degl'Innocenti and M. T. Dell'Anno, "Human and mouse cortical astrocytes: A comparative view from development to morphological and functional characterization," *Front. Neuroanat.* **17**, 1130729 (2023).
- ⁵²D. Di Lisa, L. Muzzi, S. Pepe, E. Dellacasa, M. Frega, A. Fassio, S. Martinoia, and L. Pastorino, "On the way back from 3D to 2D: Chitosan promotes adhesion and development of neuronal networks onto culture supports," *Carbohydr. Polym.* **297**, 120049 (2022).
- ⁵³T. Barra, A. Falanga, R. Bellavita, V. Laforgia, M. Prisco, S. Galdiero, and S. Valiante, "gH625-liposomes deliver PACAP through a dynamic in vitro model of the blood–brain barrier," *Front. Physiol.* **13**, 932099 (2022).
- ⁵⁴N. Marchesi, A. Barbieri, F. Fahmideh, S. Govoni, A. Ghidoni, G. Parati, E. Vanoli, A. Pascale, and L. Calvillo, "Use of dual-flow bioreactor to develop a simplified model of nervous-cardiovascular systems crosstalk: A preliminary assessment," *PLoS ONE* **15**(11), e0242627 (2020).
- ⁵⁵K. Salazar, F. Espinoza, G. Cerda-Gallardo, L. Ferrada, R. Magdalena, E. Ramírez, V. Ulloa, N. Saldivia, N. Troncoso, and M. J. Oviedo, "SVCT2 overexpression and ascorbic acid uptake increase cortical neuron differentiation, which is dependent on vitamin c recycling between neurons and astrocytes," *Antioxidants* **10**(9), 1413 (2021).